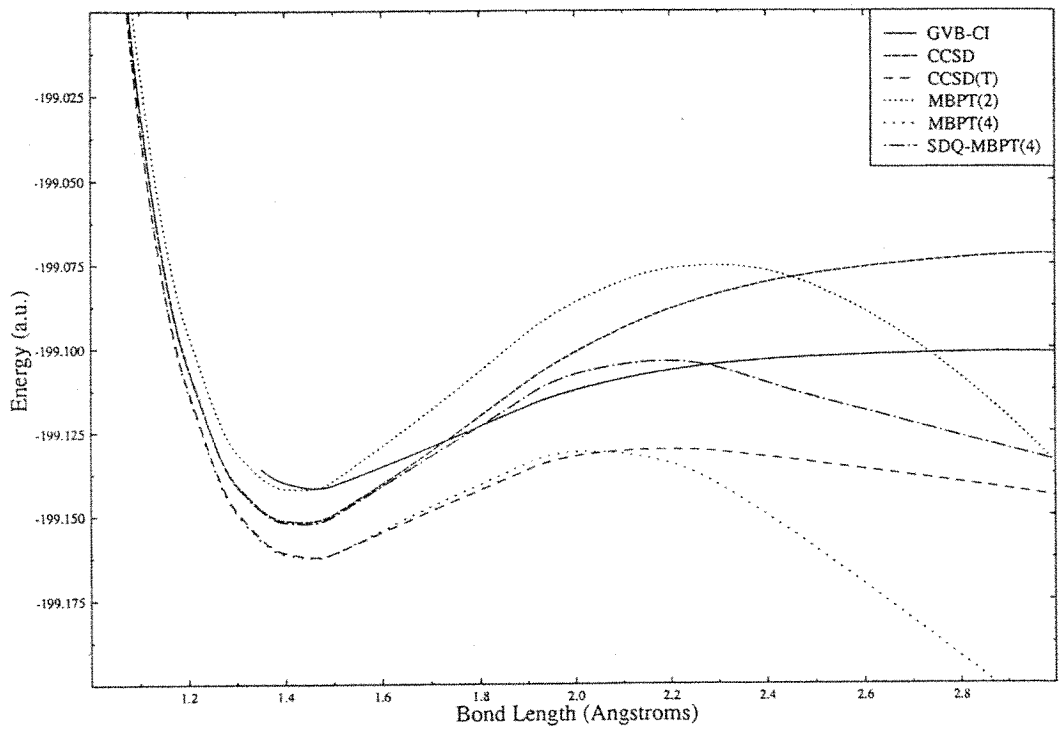

Figure 10 Correlated potential curves for F_2 using an RHF reference.

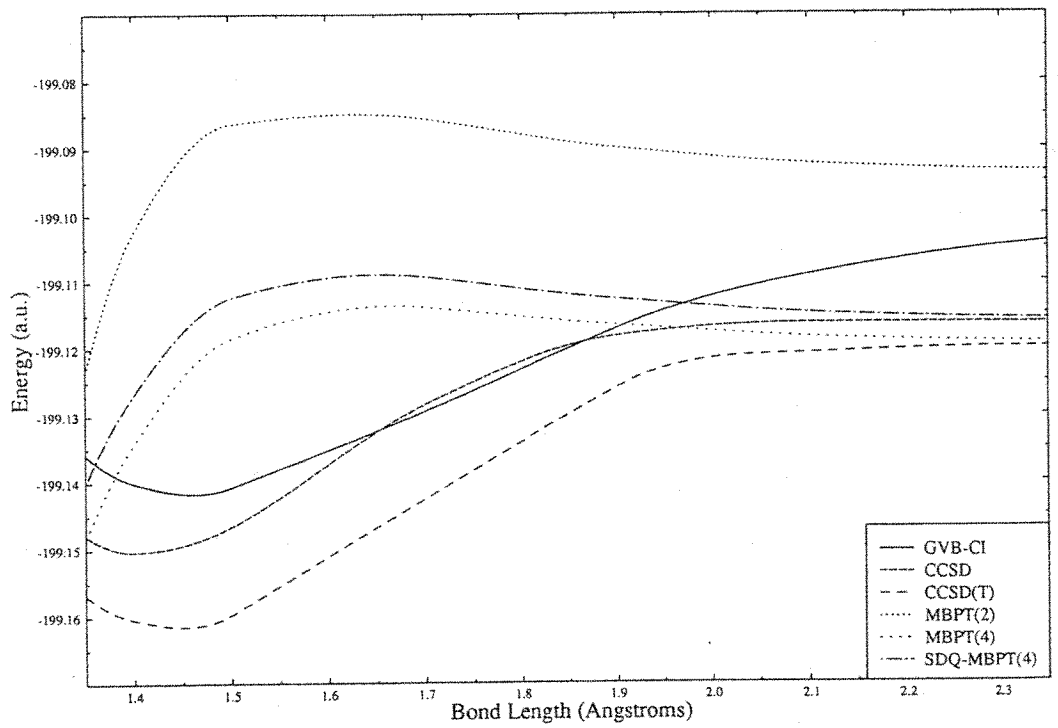

Figure 11 Correlated potential curves for F_2 using a UHF reference.

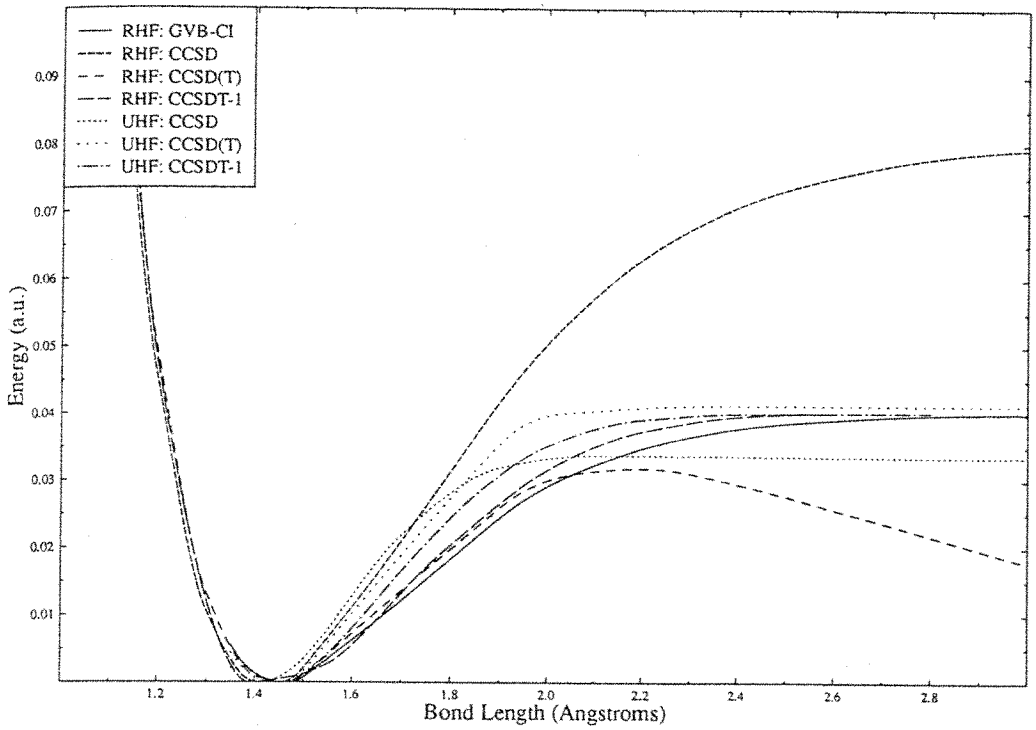

Figure 12 Correlated potential curves for F_2.

in the vicinity of equilibrium for most molecules, which is why even MBPT will usually give quite good answers. We will see many such examples in later sections.

Basis Sets

We have seen that the solution of the correlation problem within an "atomic orbital" (AO) basis set $\{\chi_\mu\}$ is given by the full CI. The full CI's agreement with experiment for various properties is a function of the choice of basis set. Since the whole mechanism for introducing electron correlation is to allow the wavefunction enough flexibility to let electrons avoid each other, the contracted Gaussian basis must include spatial flexibility.[57] This is introduced by (1) having multiple s functions for atoms that have s electrons; p functions for atoms that have p electrons, etc., and (2) by including higher angular momentum functions like d functions for B, C, O, N, F, p functions for H, f functions for the first-row transition series, etc., which are not normally required for the conceptual bonding description involving that atom. Both additions give extra flexibility to the wavefunction. Type (1) basis functions allow the correlated method to introduce "radial" correlation because we have extra flexibility in spatial regions along a bond in a molecule, while type (2) basis functions introduce polarization into the wavefunction and particularly allow for "angular correlation." While such higher angular functions will also give

improved SCF results for molecules, they are critical to the treatment of electron correlation for the obvious reason that d functions introduce areas of space that are not usually covered by s and p functions, and the more spatial flexibility, the better the electron correlation description. Similarly, f functions would introduce additional spatial flexibility, as would even higher angular momentum functions. Consequently we have to be concerned with the level of correlated theory and the quality of the basis set as shown in Table 5. The actual distance from the "truth" for a particular level of calculation and a particular property is a *"calibration"* step, largely determined by comparing results from a given level of correlated theory and basis to experiment. Calibration is discussed for several different categories of problems in later sections.

The minimum level AO basis that is meaningful for ab initio correlated treatments is at least a 6-31G*,[58] 6-31G**,[59] or, better, DZP basis.[60] The first two bases are in the GAUSSIAN program system, and the notation indicates that the core orbitals are represented by a single basis function involving a contraction of six Gaussian functions, while the valence s and p orbitals are described by two functions. The innermost, or least diffuse, function is a linear

Table 5 Basis Set Versus Quality of Theory in ab Initio Calculations

	Basis set							
Method	DZ	6-31G**	DZP	TZ2P	PVTZ	PVQZ	· · ·	Complete basis
SCF								
MBPT(2)								
CISD								
MBPT(3)								
CCD								
CCSD								
MBPT(4)								
CISDTQ								
CCSD(T)								
CCSDT								
CC5SD(TQ*)								
CCSDTQ								
MR-CI								
MR-CC								
⋮								
FULL CI								Truth

combination of three Gaussians, while the outermost is represented by a single uncontracted Gaussian. The exponents of the primitive Gaussians are the same for the valence s and p basis functions. (Many programs routinely put all six of the Cartesian components of d functions like x^2, y^2, z^2, xy, yz, xz into a calculation, and similarly 10 functions for f functions. The designation "spherical" limits the basis to the usual 5 d and 7 f functions.) The single asterisk (*) means that a set of six (Cartesian) functions is added to the heavy atom (i.e., B, C, N, O, F), while the double (**) means that a set of three p functions is added to all hydrogen atoms. Without the polarization functions, the basis sets (i.e., STO-3G, 4-31G, 6-31G, DZ, etc.) do not adequately include the most important physical effects of electron correlation. As a consequence, although there will be some energy reduction, the change will be relatively constant as a function of geometry or for ionization or excitation energies, etc., instead of introducing the physically significant differential effects of correlation.

The double zeta (DZ) basis[60] means choose twice as many s and p contracted functions as are occupied in the ground state of the atom (i.e., 2 s for H, but 4 s for Li, and 2 p for B, C, N, O, F). In practice we usually use 2 p for Be and Li, as well. The DZ plus polarization basis (DZP) means add a set of six d functions to the heavy atom and a set of three p functions to H. Unlike 6-31G**, there is no restriction to s and p contracted Gaussians having the same exponent, which gives the DZP basis additional flexibility. The primitive functions are not specified in the DZP designation, but usually the basis is derived from the 9s5p primitive optimized atomic Gaussian sets of Huzinaga.[61] This DZP basis (preferably with the polarization function exponents optimized at the correlated level for small molecules)[62] is the simplest reasonable level and will be widely used for illustrative calculations in this chapter. Obviously we could add larger primitive sets from which to define a DZP contraction, with some marginal improvement. More generally, we can use a larger contracted basis like TZP,[63] meaning 5s3p1d per atom (triple zeta in valence region), TZ2P (5s3p2d), TZ2Pf (5s3p2d1f), etc. We can use the same primitives or expanded sets. We can also add diffuse functions, which are sometimes indicated as 6-31G**++, for example.

The recently developed atomic natural orbital (ANO)[64,65] and "correlation consistent" (ccPVDZ, ccPVTZ, ccPVQZ, . . .) bases[66] use a large number of primitives and then form a contraction guided by results of correlated calculations. In the latter designation the P means polarization and the VDZ means "valence double zeta," which translates into 3s2p1d contracted Gaussians for first-row atoms, while PVTZ is 4s3p2d1f and PVQZ is 5s4p3d2f1g, etc. Even with more extensive primitive sets, the PVDZ basis tends to be slightly inferior to a DZP basis. Another useful basis is the POL1 basis of Sadlej[67] determined to accurately describe polarizabilities.

Note that for correlated calculations the number of primitive functions (n_p) is not of great concern because that number affects only the integral time (an $\sim n_p^4$ step), while the number of contracted functions $M = n + N$ deter-

mines the scale factor in correlated calculations, and that is greater than M^5. [All the integrals do not need to be transformed for MBPT(2), so then we have $\sim Mn^2N^2$ integrals.]

The larger the basis, the better the treatment of electron correlation. We cannot expect any monotonic convergence for most properties with either basis or correlated treatment, but larger basis sets and more correlation effects give methods that are "theoretically" more complete. However, the dimension of the basis is critical for post-Hartree–Fock calculations. For M contracted Gaussian (AO) functions, and n the number occupied, then $M - n = N$ unoccupied spatial orbitals left over after the SCF calculation. In typical polarized basis correlated calculations, N is more than three times the dimension of n. The cost of the SCF calculation is proportional to the number of primitive integrals $\langle \mu\nu|\lambda\delta\rangle$ (i.e., $\sim n_p^4/8$) that have to be evaluated. (For sufficiently large molecules, strategies can be exploited to make the scaling more like $\sim n_p^2$.) Regardless of what the correlated method is (CI, CC, MBPT, etc.), all such calculations start by transformating the AO two-electron integrals to the MO two-electron integrals $\langle \phi_i\phi_j|\phi_k\phi_l\rangle$. This requires a procedure proportional to $\sim M^5/4$. Molecular symmetry can be exploited to reduce the cost of integral evaluation by h, where h is the order of the point group, e.g., $h = 8$ for D_{2h}, and the integral transformation by a factor of h^2. CISD, CCSD and MBPT(3) require an n^2N^4 step, while other widely used higher order methods like MBPT(4) and CCSD(T) are $\sim n^3N^4$. By using molecular symmetry, all such methods with the exception of MBPT(2) can be reduced by a factor of h^2, which can result in a critical savings for large-scale correlated calculations.[68] Despite the advantages of symmetry when applicable, the nonlinear dependence on N (which even for a DZP basis is typically a factor 3–4 times n; for a TZP basis the factor is $\sim 5n$ and TZ2P, about $\sim 6n$, etc.) seriously impedes our ability to do correlated calculations. Doubling the size of the basis set requires $\sim 2^3$ as much computer time for MBPT(2), $\sim 2^4$ for MBPT(3), CCSD or CISD and $\sim 2^5$ for MBPT(4) or CCSD(T).

The nonlinear dependence on basis size greatly limits either the size of molecule or the basis set in a correlated calculation. To help some, inner shell electrons, which are known to have little effect on the formation of chemical bonds, are frequently not correlated. This means that the lowest occupied orbital (largely the 1s core AO) and the corresponding virtual orbital (V1s) are deleted from the basis before making the correlated calculation. For CH_4, this saves just two functions, but for C_6H_6, it would be 12. Similarly, for systems containing heavier atoms like Fe, several lower orbitals like 1s, 2s, and 2p can frequently be left uncorrelated without serious error. That usually means deleting the V1s, V2s, and V2p orbitals as well, because their primary function is to correlate the core orbitals; so 10 orbitals would be dropped from the correlated calculation. Most programs allow the automatic exclusion of such orbitals prior to the transformation for the correlated calculation.

Another option that reduces the number of functions, particularly when heavy atoms are involved, is the replacement of inner shell electrons by effective (or pseudo) potentials.[69] Such procedures have been incorporated into many ab initio program systems including ACES II. Since the core electrons are not explicitly considered, effective potentials can drastically reduce the computational effort demanded by the integral evaluation. However, because the $\sim n_p^4$ step is an inexpensive part of a correlated calculation, the role of effective potentials in correlated calculations is less important, due to the fact that dropping orbitals is tantamount to excluding them via effective potentials. An exception occurs when relativistic effects are important, as they would be in a description of heavy atom systems. Most such chemically relevant effects are due to inner shell electrons; their important physical effects, like expanding the Pt valence shell, can be introduced via effective potentials that are extracted from Dirac–Fock or other relativistic calculations on atoms.[70] Similarly, some effective potentials introduce some spin-orbital effects as well.[71] Thus, besides simplifying the computation, effective potential calculations could include important physical effects absent from the ordinary nonrelativistic methods routinely applied.

MOLECULAR GEOMETRIES

Because the concept of structure is central to chemistry, it is only natural that prediction of molecular geometries has historically been the most frequent area of application for quantum chemical methods. For the most part, these studies can be loosely grouped into two categories. In the first, rather general questions of structure are addressed, such as the point group symmetry of the molecule (e.g., is cyclobutadiene D_{2h} or D_{4h}?). Other investigations are directed toward predictions of the fine details of structure (bond lengths, bond angles, torsional angles, etc.), and it is this second group we discuss here.

Unlike some of the topics addressed in this chapter, the study of molecular geometries does not force us to explicitly consider more than one electronic state. Hence, correlation effects do not involve unpredictable differential correlation between states, but rather only changes in the correlation energy as one moves along the potential energy surface. As it turns out, the qualitative effects of correlation on geometrical structures tend to be systematic.

A definition of molecular structure is actually fairly complicated. For the most part, we tend to view this question from a classical perspective in which structure is defined by an arrangement of nuclei that minimizes the potential energy. The geometrical parameters that characterize these special points on the potential energy surface constitute an "equilibrium structure," where forces on the atoms vanish (i.e., $\partial E/\partial X_\alpha = 0$ for all Cartesian coordinates X_α). This is

the geometry the molecule might assume in the absence of available energy. However, in the real (quantum mechanical) world, molecules are never at rest and molecular structure is a dynamical concept involving oscillations of the nuclear positions about equilibrium geometries.

While quantum chemists typically calculate equilibrium geometries, experimentalists can only measure average structures in a direct fashion. For example, rotational spectroscopy yields moments of inertia that are related to average geometries in specific vibrational states, whereas electron diffraction provides internuclear distances averaged over a statistical ensemble of vibrational and rotational states. Extraction of equilibrium geometries from experimental data is an exceedingly difficult task for all but diatomic molecules because the anharmonic force field of the molecule must be known. Reliable equilibrium geometries are available for several triatomic molecules and a scant number of larger systems. For the most part, however, differences between equilibrium and vibrationally averaged structures are small ($\leq$0.01 Å for bond lengths, $\leq 0.5°$ for angles), and it is therefore possible to make meaningful comparisons between theoretical calculations and experimental results, provided we are careful.

The determination of equilibrium geometries involves the location of minima on the potential energy surface. At such a point, all first derivatives of the energy vanish (i.e., there is no net force on the nuclei) and the matrix of second derivatives (the Hessian) has no negative eigenvalues. For small molecules (particularly diatomics and triatomics), the potential energy surface is of small dimension, and it is not difficult to locate stationary points. Even the relatively crude procedure of evaluating the energy over a grid of points followed by interpolation works well. However, as molecular size grows, the potential surface rapidly becomes complex and more sophisticated approaches are warranted.

The intractability of simple energy-grid-based approaches is most easily communicated by means of an example. Suppose that one wanted to determine the equilibrium structure of 3-fluorotoluene. Even if C_s symmetry is imposed, there are still 22 distinct degrees of conformational freedom for the molecule. Consequently, if we want to perform a Newton–Raphson step to improve the geometry, we will have to determine the 22 components of the gradient and 253 unique Hessian elements. To calculate the derivatives with sufficient numerical accuracy, so-called double-sided differentiation must be used. (Such a procedure, which means taking equal $+\delta_q$ and $-\delta_q$ displacements for derivatives, removes the contaminating effects of the next higher derivatives and therefore improves numerical accuracy.) This would require that a grid of ~500 energy points be evaluated, which is clearly not a practical procedure! However, a number of useful numerical techniques exist that allow us to estimate the Hessian, based on information from preceding geometry steps. Thus, it is practical to begin with a reasonable estimate of the Hessian and evaluate only

the first derivatives. Nevertheless, a numerical evaluation of the gradient by the double-sided method

$$\left.\frac{\partial E}{\partial q_i}\right|_{q_i=q_0} = \frac{E(q_0 + \delta) - E(q_0 - \delta)}{2\delta} \qquad [47]$$

requires 44 energy calculations.

The bottleneck in geometry optimizations alluded to above has yielded to one of the most important advances in quantum chemistry—the development of methods to calculate the gradient of the energy analytically.[72-76] An efficient formalism for the calculation of SCF derivatives was developed more than 20 years ago, and the first analytic derivative formulation for correlated methods followed a decade later. For the MBPT and CC approaches advocated by us, analytic gradient methods have been implemented for all the computational levels typically used in practice—MBPT(2), MBPT(3), SDQ-MBPT(4), MBPT(4), CCD, CCSD, CCSD + T(CCSD), CCSD(T), QCISD, and QCISD(T).[77-83] The ACES II program system allows the routine calculation of gradients at all these levels for both RHF and UHF reference functions, while ROHF-based MBPT(2),[80] CCSD,[79] and CCSD(T)[83] derivatives are also available. Other program packages permit analytic evaluation of UHF and RHF-based MBPT(2) derivatives and RHF-CISD, although no package other than ACES II has CC/MBPT gradient capabilities beyond MBPT(2). The GAUSSIAN program system is capable of evaluating gradients at the QCISD level.

In general, analytic gradient calculations scale only weakly with the number of degrees of freedom and typically require roughly 1–3 times the CPU time as the energy calculation itself. Gradients for SCF and correlated methods may be evaluated from the formula

$$\frac{\partial E}{\partial X_\alpha} = \mathrm{Tr}\left(\frac{\partial H}{\partial X_\alpha}\rho\right) + \mathrm{Tr}\left(\frac{\partial S}{\partial X_\alpha} I\right) \qquad [48]$$

where $\partial H/\partial X_\alpha$ is a derivative of the Hamiltonian matrix for one of the $3N$ Cartesian coordinates, ρ is a suitably defined density matrix, $\partial S/\partial X_\alpha$ are the derivatives of the overlap integrals, which serve to preserve the orthonormality of the wavefunction, and I is a one-particle-like quantity.

For SCF methods, ρ represents elements of the one- and two-particle density matrices. In correlated methods, the one-particle part of ρ is the sum of the actual reduced density and a contribution that is proportional to the derivative of the energy with respect to orbital rotations. For the MCSCF method, the orbitals are variationally optimum, and this latter term vanishes. Similarly, for FCI there is no orbital contribution. However, it is required for other CI, CC, and MBPT correlated methods, because the energy in these approaches is not stationary with respect to first-order changes in the molecular orbitals. This

latter term is said to account for "orbital relaxation," and the composite ρ is called a "relaxed" or "effective" density. Hence, all gradient calculations consist of evaluating density matrices and I intermediates and contracting them with matrix elements of an appropriately differentiated operator. For SCF methods, construction of ρ and I involves negligible computational expense, and timings are therefore dominated by integral derivative evaluation, which typically requires about twice the CPU time as the calculation of undifferentiated integrals.

For MBPT and CC methods, evaluation of the reduced density requires determining a response vector (Λ) as well as T. This defines a response density $\rho' = e^T|\Phi_0\rangle\langle\Phi_0|(1 + \Lambda)e^{-T}$. In addition, we want to allow the molecular orbitals to relax. The latter consideration adds another term, ρ'', to the one-particle density. This "relaxed" density, $\rho = \rho' + \rho''$, is the critical quantity in CC and MBPT analytical gradient (and property) methods.[84] For just the one-particle part, we have $\rho(1) = \rho'(1) + \rho'' = D(1)$ which will show up again when we discuss properties.

For all methods besides MBPT(2) and MBPT(3), the evaluation of Λ requires a fair amount of additional computation. However, even for CC methods this step requires only about half the CPU time of the CC calculation itself. Hence, for calculations in which the integral evaluation time is negligible the ratio of timings between MBPT/CC energy and energy plus gradient calculations is expected to be between ~1:1 and 1:1.75. Thus, it may be seen that the availability of efficient analytic gradient methods greatly facilitates the study of potential energy surfaces. Indeed, the development of such techniques now seems to be a prerequisite for any method intended for use in chemical applications.

The accuracy of molecular geometries predicted by the SCF approximation has received considerable attention in the literature. On the whole, the neglect of electron correlation causes bond lengths to be underestimated, as seen in the basis set study for water in Table 6. This statement about underestimated bond lengths applies to exact SCF calculations, namely those in which the basis set is complete. As seen in Table 6, SCF calculations performed with

Table 6 Optimized SCF Molecular Geometry Data for H_2O as a Function of Basis Set

Basis	R_e, O—H (Å)	θ, H–O–H (degrees)
STO-3G	0.989	100.0
3-21G	0.967	107.7
DZ	0.951	112.5
6-31G*	0.947	105.5
DZP	0.944	106.6
TZ2P	0.941	106.2
Experimental	0.957	104.5

poor basis sets often overestimate the distance between bonded atoms. The underestimation, of course, is a manifestation of deficiencies of the SCF model for potential energy surfaces discussed previously. In SCF calculations, the electron–electron repulsion terms are not treated properly, and electrons tend to bunch together too closely. This results in compact bonds with favorable Coulombic attractions between the electrons and nuclei. However, when interelectronic repulsion is treated properly, the electrons move apart, which causes the bond lengths to increase. The overestimation of bond angles observed in SCF calculations for many molecules may be rationalized as a consequence of the considerations discussed above. That is, underestimation of the bonded distances causes an increased (and unfavorable) interaction between the nonbonded atoms. Therefore, bond angles increase.

Another ubiquitous trend in SCF geometry studies, which is illustrated by the data in Table 6 is a marked inverse relationship between the quality of the basis set and the predicted bond lengths. In our water example, SCF bond lengths monotonically decrease from 0.989 Å to 0.941 Å as the basis set is improved from STO-3G to TZ2P. In water as well as many other molecules, small basis sets usually overestimate the experimental bond lengths, which are in turn longer than those obtained at the SCF level with extensive basis sets. Therefore, it is often possible to select a basis set of intermediate quality (DZ in the present example) which gives an accurate "prediction" of R_e. This is an example of a *Pauling point*—a level of theory that provides better results than those obtained in more sophisticated calculations—and is due to the opposing nature of correlation and basis set corrections, which tend to increase and decrease bonded distances, respectively. [This situation should contrast with the calculation of excitation energies, in which both correlation and basis set effects tend to act in concert with improvements in both leading to lower values (see later).] Indeed, SCF geometry optimizations in a split-valence polarized basis set, such as 3-21G or DZ, have long been used to predict geometries of organic molecules. For the most part, this approach works reasonably well, because the errors tend to be highly systematic provided lone-pair electrons are not present. However, the results for our water example clearly illustrate that polarization functions are needed to predict bond angles, so one must exercise a certain amount of care in choosing basis sets for geometry optimizations. It is very difficult to predict the location of Pauling points a priori; instead *one must rely on experience gained in studies of similar molecules.* For example, one should not expect the equilibrium bond length of ozone predicted at the SCF level with a DZ basis set to be as accurate as that for the O—H bond in water. Indeed, at the DZ-SCF level the equilibrium for ozone is predicted to be R_e(O—O) = 1.259 Å; θ = 119.7°, as compared to the experimental results of 1.272 Å and 116.8°, respectively. Whereas our experience for water is consistent with the overestimation of the bond angle with this unpolarized basis set, the error in bond length (−0.012 Å) is about twice that found for water (−0.006 Å).

The only reliable way to obtain molecular structures that converge toward the correct result is to use increasingly larger basis sets and more complete treatments of electron correlation. For water, the results of calculations using a variety of basis sets (STO-3G, 3-21G, DZ, 6-31G*, DZP, and TZ2P) and computational methods [SCF, MBPT(2), CCSD, and CCSD(T)] are listed in Table 7. The equilibrium bond lengths and bond angles predicted by these calculations clearly demonstrate the trends discussed above, namely the tendency for electron correlation to increase bond lengths (and by consequence reduce bond angles), while basis set expansion exhibits the opposite behavior. Nevertheless, the magnitudes of the changes are relatively modest once a reasonable level of theory has been surpassed, such as MBPT(2) with the DZP basis set.

Having results obtained at a few correlated levels with different basis sets, it is usually possible to estimate the direction of the residual error with a fair degree of confidence. As an example, let us consider water once again. Because water has a well-isolated electronic ground state and no significant nondynamical electron correlation effects, the CCSD(T) approximation should provide a nearly quantitative treatment of correlation. Hence, the error in our most sophisticated calculation [CCSD(T) with the TZ2P basis set] should be due almost entirely to deficiencies in the basis. The structure obtained in this calculation [R_e (O—H) = 0.959 Å and θ = 104.2°] is therefore expected to have an overestimated bond length and underestimated bond angle, as verified by comparison with the experimental values.

In Table 8, we list errors in bond length (Å) and bond angles (degrees) calculated at various correlated levels with a DZP basis set for a set of molecules. The equilibrium geometries of the systems studied here have been reasonably well determined experimentally, so comparisons between the present values and the experimental results are relevant.

The effects of correlation (Table 8) exhibit the same qualitative behavior we have noted for water. (One should note that the rationalization provided for the behavior of the bond angle in water does not apply to formaldehyde,

Table 7 Optimized Geometries (in angstroms and degrees) for H_2O as a Function of Basis Set

	SCF		MBPT(2)		CCSD		CCSD(T)	
Basis	R_e	θ	R_e	θ	R_e	θ	R_e	θ
STO-3G	0.989	100.0	1.013	97.3	1.028	96.8	1.028	96.8
3-21G	0.967	107.7	0.989	105.2	0.993	104.9	0.994	104.8
DZ	0.951	112.5	0.979	110.5	0.979	110.3	0.980	110.3
6-31G*	0.947	105.5	0.969	104.0	0.969	104.0	0.971	103.9
DZP	0.944	106.6	0.963	104.4	0.961	103.7	0.962	103.6
TZ2P	0.941	106.3	0.958	104.2	0.956	104.5	0.959	104.2
Experimental							0.957	104.5

Table 8 Errors in Bond Lengths and Angles for Various Levels of Theory (DZP Basis)

SCF	MBPT(2)[a]	SDQ-MBPT(4)[a]	CCSD[b]	MBPT(4)[a]	CCSD(T)[c]	Molecule	Bond or angle
			Bond lengths (Å)				
−0.006	0.005	0.004	0.004	0.005	0.005	H_2O	OH
−0.011	0.002	0.003	0.003	0.004	0.004	NH_3	NH
−0.001	0.003	0.005	0.005	0.006	0.006	CH_4	CH
−0.002	0.006	0.006	0.007	0.008	0.008	C_2H_2	CH
−0.012	0.024	0.017	0.016	0.025	0.023		CC
−0.005	0.003	0.004	0.004	0.008	0.006	CH_2O	CH
−0.015	0.022	0.017	0.015	0.023	0.021		CO
−0.003	0.004	0.005	0.005	0.006	0.006	HCN	CH
−0.017	0.032	0.020	0.019	0.030	0.024		CN
−0.008	0.007	0.005	0.006	0.007	0.008	HNC	NH
−0.010	0.025	0.020	0.017	0.031	0.024		CN
−0.015	0.022	0.016	0.012	0.028	0.018	CO_2	CO
			Average absolute error				
−0.009	0.013	0.010	0.009	0.015	0.013		
			Bond angles (degrees)				
2.1	−0.1	0.1	0.1	0.0	0.0	H_2O	H–O–H
1.5	0.0	−0.2	−0.2	−0.3	−0.4	NH_3	H–N–H
−0.3	−0.2	−0.3	−0.2	−0.6	−0.2	CH_2O	H–C–O
			Average absolute error				
1.3	0.1	0.2	0.2	0.3	0.2		

[a] Reference 85.
[b] Reference 86.
[c] Reference 87.

because variation of the H–C–H bond angle involves changes in three distinct nonbonded interactions.) Due to the nature of the basis set used in these calculations, the bond lengths obtained with the most sophisticated treatment of correlation [CCSD(T)] are systematically longer than the experimental values. Absolute errors in bond length are largest for multiple bonds (CN, CC, and CO) at both the SCF and correlated levels. Assuming that the majority of error in the CCSD(T) results is due to basis set deficiencies, this observation suggests that both basis set and correlation effects are more pronounced for multiple bonds than for single bonds as discussed previously. The basis set sensitivity results from the more pronounced correlation effects, because larger basis sets provide a more flexible set of the virtual orbitals required to describe correlation. This reflects a statement made early in this chapter. To paraphrase: *when correlation effects are important, a large basis set is needed to describe them properly!* This is one of the important messages we are trying to convey.

We conclude this section with a brief discussion on a related topic—the optimization of transition state structures at the correlated level. In these calculations, the stationary points of interest are those that have precisely one significant negative eigenvalue of the Hessian matrix. Such points always represent the energy maximum along a minimum energy pathway linking two local minima on the potential energy surface. Points with more than one negative eigenvalue never represent transition states because there is always a lower energy path between the minima. In some sense, these other points (which are only of academic interest) represent transition states between transition states. Location of saddle points on potential energy surfaces is more difficult than finding local minima. However, a number of clever algorithms have been developed in the past decade.[88,89]

As chemical reactions proceed via pathways that are either allowed or disallowed by orbital symmetry considerations,[90] studies of transition states may also be broadly categorized in this way. In the former case, orbitals of the reactants map smoothly into those of the products and MBPT/CC calculations based on a single determinant reference should therefore be appropriate for studying the reaction pathway. However, for "forbidden" reactions, the region of the potential energy surface near the transition state is usually very poorly described by a single determinant starting point, and multi-reference-based methods are warranted. Many interesting chemical reactions (particularly those with low barrier heights) are allowed by orbital symmetry, and the single reference correlated methods discussed in this chapter may readily be applied to a study of these reactions.

A prototypical example of a transition state amenable to single determinant MBPT/CC methods is the unimolecular dissociation of formaldehyde

$$CH_2O \rightarrow H_2 + CO \qquad [49]$$

which has been the subject of a number of theoretical and experimental studies. Structural parameters of the transition state calculated with a DZP basis and a

Table 9 Internal Coordinates (in angstroms and degrees) for the Transition State in the Decomposition of Formaldehyde

Correlation treatment	$R(CO)$	$R(CH_1)$	$R(CH_2)$	$\theta(OCH_2)$	$\theta(H_2CH_1)$
SCF	1.151	1.102	1.583	112.5	49.4
MBPT(2)	1.192	1.096	1.596	111.6	50.7
CCSD	1.188	1.094	1.595	110.2	51.4
CCSD(T)	1.193	1.092	1.621	110.3	52.2

number of different treatments of correlation are listed in Table 9. For topological features of molecules that are common to both reactants and products, the considerations of basis set and correlation effects discussed earlier in this section still apply. For example, in the formaldehyde decomposition reaction, the C—O bond length increases from 1.151 Å to 1.193 Å as the level of theory is increased from SCF to CCSD(T). The magnitude of this expansion (0.042 Å) is comparable to that found for the C—O bond in ground state formaldehyde using the same basis (0.035 Å). However, the simple systematic behavior we have observed for ground state structures usually does not hold for bonds that are broken or otherwise transformed by the reaction. In this transition state, for example, the two C—H distances behave quite differently as the treatment of correlation is improved. With respect to the SCF structure, the distance between the carbon and the proximal hydrogen actually decreases by 0.010 Å while the other C—H distance increases by 0.038 Å at the CCSD(T) level.

VIBRATIONAL SPECTRA

For rigid molecules, energy differences between the ground and singly excited vibrational states are relatively small with respect to barrier heights on the potential energy surface. Hence, the nuclei tend to undergo only small-amplitude vibrations about their equilibrium positions in both the ground and excited states and therefore do not sample a large region of the potential surface. As a result, the part of the potential energy surface that governs these states and the transitions between them can be reasonably approximated by the potential function of a multidimensional harmonic oscillator. In the theory of vibrational spectroscopy, this "harmonic" approximation plays a role similar to that of the Hartree–Fock approximation in electronic structure theory. Both these simplifying approximations lead to separable and therefore exactly soluble Schrödinger equations, the solutions of which ("normal" vibrational modes and molecular orbitals, respectively) represent useful paradigms for our understanding of the respective phenomena. However, we must be careful to remember that both normal coordinate theory and molecular orbital theory are approximations, and exact calculations must go beyond these models.

Because of the properties noted above, most quantum chemical studies of vibrational frequencies are carried out within the "double" harmonic approximation (i.e., using only second derivatives for the force constants and the derivative of the dipole moment for the intensities; see below). This neglects the so-called mechanical and electrical anharmonicities. As is the case for theoretical predictions of molecular structures, we must once again be careful when comparing experimental and theoretical results. In structural predictions, one is usually forced to compare equilibrium geometries obtained by theory to some sort of averaged geometry obtained from experiment, whereas vibrational calculations produce harmonic frequencies that do not include anharmonic effects. Hence, to rigorously assess the quality of harmonic force fields obtained theoretically, it is necessary to compare results to "experimental harmonic frequencies." We believe that the difficulty of obtaining harmonic frequencies experimentally is not as widely appreciated among the quantum chemical community as it should be. Indeed, the amount of information required to determine harmonic frequencies from experimental data is the same as that needed to determine the equilibrium geometry. Therefore, the number of systems for which accurate harmonic frequencies have been determined is even smaller than that for which the equilibrium geometry is known with precision. The point of this section is to assess how accurately different quantum chemical methods can predict harmonic frequencies, so we will concern ourselves primarily with such systems.

The quantities we require in a calculation of harmonic vibrational frequencies are the second derivatives (i.e., the force constants) of the electronic energy with respect to nuclear displacement, $\partial^2 E/\partial q_\alpha \partial q_\beta$. In terms of Cartesian coordinates there are $3N$ such terms, for N atoms. Elimination of translational and rotational degrees of freedom gives the familiar $3N - 6(5)$ independent nuclear coordinates. We refer to the force constant matrix as the Hessian matrix. The eigenvalues of the Hessian matrix must all be positive at a minimum energy geometry, while at a transition state (which corresponds to a saddle point), one will be negative. The corresponding eigenvector identifies the reaction path, while the remaining eigenvalues are positive. Operationally, we can evaluate second derivatives of the electronic energy in one of three ways:

1. Obtain the energy at several points and determine the second derivatives from numerical second derivatives. If we insist on "double-sided" numerical differentiations, which is recommended because it benefits from eliminating any third-derivative contaminant, we require $E(0)$ and $E(\pm\delta q_\alpha)$ for each Cartesian displacement, δq_α. Clearly, symmetry can be used to reduce the number of calculations by replacing q_α by symmetry coordinates (S_α). This is done automatically in ACES II.
2. Evaluate the gradient to provide analytic first derivatives $\{\partial E/\partial q_\alpha\}$ from which $\partial^2 E/\partial q_\alpha \partial q_\beta$ can be obtained by a displacement in $\pm\delta q_\beta$. Again, symmetry can be exploited to reduce the number of gradient evaluations.
3. Evaluate the second derivative matrix analytically.

Each level is more efficient and numerically accurate than the preceding one. For most polyatomic molecules, ab initio calculations using approach 1 are not feasible because of the large number of independent degrees of freedom: they require roughly $(3N - 6) \times (3N - 5)/2 \times 2$ energy calculations. Approach 2 is used for many applications of interest at correlated levels. Approach 3 is readily used in SCF calculations, and although some attempts have been made for MCSCF, CI, and CCSD methods; in practice, correlated analytical Hessians have been largely limited to MBPT(2).[91-93] Analytic MBPT(2) Hessian evaluation for RHF,[91] UHF,[92] and ROHF[93] reference functions have now been presented and will be available in ACES II.

At uncorrelated levels, the frequently incorrect separation of the RHF wavefunction or spin contamination in a UHF solution will cause too large a curvature, illustrated in the diatomic potential curves discussed earlier. Hence, SCF will normally overestimate the second derivatives, causing the resultant harmonic frequencies to be too high. (Note that pathological situations, such as the UHF curve for F_2 and "symmetry breaking" where the RHF, ROHF, or UHF solution for some small displacement fails to connect to that at the higher symmetry point, have to be recognized. The latter frequently prohibits calculating second derivatives with finite displacement, although analytical second derivatives can be obtained at the high symmetry point.) The SCF-predicted frequencies are found to be about 10% above the fundamental vibrational frequencies observed experimentally, recommending an *empirical scaling factor* of 0.9. Some workers use different scale factors for different frequency modes (symmetric stretches, asymmetric stretches, bends, etc.) or applied to the force constants for these modes. We show the differences between experimental harmonic frequencies and DZP basis SCF theory for several ordinary closed-shell molecules in Table 10. Also in Table 10 are results from several different levels of electron correlation. Any level of electron correlation reduces the SCF error to about 5%. (In this table, the "experimental" values correspond to actual harmonic frequencies, but the reader should remember that these are rarely available for polyatomic molecules.) Most of the error is recovered at the simplest MBPT(2) level, with more modest improvements at higher levels.

In terms of computational requirements, MBPT(2) is a highly applicable level of correlated theory. The results are somewhat better than the infinite-order CISD. Unlike CISD, MBPT(2) is an extensive method, and that means that even though it corresponds to the first iteration of CISD, it is also the first iteration of CCSD, and it tends to give results closer to those for CCSD than for CISD. Second, as discussed previously, MBPT(2) tends to overestimate bond lengths and angles compared to experiment. Because longer bonds tend to diminish the force constants, MBPT(2) vibrational frequencies usually move closer to experimental values. That, together with the ready availability of analytical Hessians, makes MBPT(2) a highly useful method for extensive (!) applications to molecules.

Concerning the scaling of the SCF frequencies, another point should be made. An implicit assumption underlying the use of empirical scaling factors is

Table 10 Differences Between Theoretical and Experimental Harmonic Frequencies ω (cm^{-1}) for Several Small Molecules (DZP Basis)

Molecule		Experimental	SCF[a]	CISD[a]	MBPT(2)[b]	SDQ-MBPT(4)[b]	CCSD[a]	MBPT(4)[b]	CCSD(T)[c]
H_2O	ω_1	3832	332	135	77	89	80	73	64
	ω_2	1649	102	44	15	33	34	26	28
	ω_3	3943	344	147	112	107	98	92	83
NH_3	ω_1	3506	218	91	67	56	45	40	27
	ω_2	1022	97	98	78	97	97	99	100
	ω_3	3577	295	165	164	135	123	121	107
	ω_4	1691	111	204	12	27	25	20	18
CH_4	ω_1	3026	148	90	86	71	61	62	50
	ω_2	1583	88	18	11	5	3	−1	−4
	ω_3	3157	137	100	117	85	73	77	63
	ω_4	1367	90	30	16	20	18	14	11
C_2H_2	ω_1	3497	84	94	54	53	41	30	22
	ω_2	2011	194	70	−58	3	8	−60	−29
	ω_3	3415	162	77	49	40	28	23	10
	ω_4	624	146	−4	−78	−58	−61	−109	−106
	ω_5	747	116	22	−16	−10	−13	−35	−37
H_2CO	ω_1	2978	171	102	62	47	51	19	26
	ω_2	1778	228	99	−8	28	41	−26	3

	ω_3	1529	127	71	39	41	44	19	30
	ω_4	1191	144	56	23	21	20	4	1
	ω_5	2997	229	165	132	108	113	78	88
	ω_6	1299	68	11	−18	−14	−12	−30	−24
HCN	ω_1	3440	196	109	64	61	53	35	31
	ω_2	2128	276	96	−131	−15	17	−119	−25
	ω_3	727	131	35	−11	0	−1	−28	−35
CO_2	ω_1	1354	159	75	−28	−10	25	−95	−13
	ω_2	2397	193	116	59	27	51	−28	−12
	ω_3	673	94	37	−17	−2	9	−38	21
C_2H_4	ω_1	3139	191		108	172		159	
	ω_2	1655	165		44	57		32	
	ω_3	1371	101		21	21		6	
	ω_4	1047	87		18	5		−5	
	ω_5	3212	183		120	99		7	
	ω_6	1245	94		15	20		10	
	ω_7	968	113		−9	−12		−29	
	ω_8	959	130		−148	−130		−172	
	ω_9	3234	187		126	105		92	
	ω_{10}	843	47		−12	−10		−18	
	ω_{11}	3138	165		85	72		57	
	ω_{12}	1473	113		33	40		30	
Error, %			8.7	3.7	3.2	2.5	2.2	3.1	2.4

[a] Reference 86.
[b] Reference 85.
[c] Reference 87.

that the order of the vibrational frequencies is correctly predicted at the SCF level. However, for many molecules, correlation effects interchange the order, as illustrated by C_2H_4 in Table 10. Experimentally, the $\omega_7(b_{1u})$ mode has a higher frequency than $\omega_8(b_{2u})$, but SCF has the reverse ordering. MBPT(2) and all higher correlated levels have the correct order. This also seems to be a characteristic of several proposed nitrogen analogs of cyclopropane and cyclopentadiene, N_3H_3[94] and N_5H,[95] where the SCF order (and intensities) are significantly changed at the MBPT(2) level. MBPT(2) is not always right, however, as unwarranted changes from SCF for the open-shell OCBO molecule[96] were rectified at higher order CC levels.

In addition to the frequencies, the infrared intensities may be determined by evaluating $\partial\mu_i/\partial X_\alpha$ where μ_i is a component of the dipole moment and X_α is a Cartesian nuclear displacement. The dipole moment itself can be viewed as the gradient of the electronic energy with respect to an electric field ϵ_i (see later discussion of molecular properties), so $\partial\mu_i/\partial X_\alpha = \partial^2 E/\partial\epsilon_i\partial X_\alpha$ requires a cross-second derivative. Just as for force constants, analytical evaluation is preferred and is now routine for MBPT(2). For higher correlated methods, analytical evaluation of μ_i from the relaxed density at finite nuclear displacements is used to obtain the intensities. Whereas the calculated frequencies only are subject to the accuracy of the energy as a function of displacement, intensities are more sensitive to diffuse regions of the electronic density through the dipole matrix elements, placing greater demands on the quality of the basis set.[97,98]

Mean absolute errors for IR intensities determined from the standard molecules discussed above are shown in Table 11 for different levels of approximation and a DZP basis. Of course, errors for relative intensities are much smaller.

Once again, it appears that for a modest basis set like DZP, MBPT(2) is on average about as good as more sophisticated correlated methods. This does not necessarily follow once the basis has been improved, however. To illustrate this we present frequencies and intensities with DZ, DZP, and TZ2P basis sets for H_2O in Table 12. As the level of correlation and basis are improved, there is a fairly regular convergence toward the experimental values. In particular,

Table 11 Errors in Intensities at Various Levels of Theory (DZP Basis)[a]

Method	Mean absolute error (%)
SCF	96
MBPT(2)	41
CISD	47
SDQ-MBPT(4)	34
CCSD	41
MBPT(4)	40
CCSD(T)	34

[a]Extracted from same references as in Table 10.

Table 12 Vibrational Frequencies (cm^{-1}) and Intensities (km mol^{-1}) for H_2O as a Function of Basis Set

Basis sets	ω_1	ω_2	ω_3	I_1	I_2	I_3
DZ						
SCF	4028	1711	4204	3.4	135.8	65.0
MBPT(2)	3674	1624	3872	0.4	100.4	27.0
SDQ-MBPT(4)	3668	1638	3848	1.7	95.1	15.3
CCSD	3653	1639	3831	2.2	93.6	13.0
DZP						
SCF	4164	1751	4287	20.5	108.0	73.8
MBPT(2)	3909	1664	4055	4.5	80.9	45.6
SDQ-MBPT(4)	3905	1687	4020	5.9	65.8	30.7
CCSD	3898	1687	4012	5.6	65.9	29.8
CCSD(T)	3879	1681	3994	4.3	63.5	26.6
TZ2P						
SCF	4133	1752	4237	20.9	88.0	98.7
MBPT(2)	3864	1653	3987	10.6	61.6	77.5
SDQ-MBPT(4)	3883	1678	3991	8.0	62.7	61.3
CCSD	3886	1679	3991	8.0	63.4	61.0
CCSD(T)	3848	1670	3955	6.4	60.1	56.1
Experimental	3832	1649	3943	2.2	53.6	44.6

larger basis sets with higher level correlated methods generally show significant improvement over MBPT(2). In the case of the symmetric stretch mode ω_1 the small "experimental" value for I_1 is likely to be as much in error as the calculation, so the error value might not be too meaningful. In fact, several other "experimental" values are available for these intensities.

Table 13 shows a few more examples of results using a larger TZ2Pf basis,[99] that contains f functions.[100] The average error for CCSD(T) results for frequencies is 0.7%, while the intensities have an average absolute error of 16%.

The customary accuracy of MBPT(2) has now been extended to purely analytical second-derivative methods for open shells using UHF[93] or ROHF reference functions. The latter requires some new (noncanonical MBPT/CC) theory recently developed.[80,93] As discussed previously, unlike ROHF, which is an eigenfunction of spin for high spin cases, UHF reference functions can sometimes suffer from spin contamination. For low order correlated methods like MBPT(2) (unlike CCSD, e.g.), the UHF spin contamination can drastically affect the answers obtained.

As an example, consider the methylene imidogen molecule, CH_2N.[93] This system, which is isoelectronic with the vinyl radical, has a multiplicity $2S + 1 = 2.256$ at the UHF level. Its vibrational frequencies are shown in Table 14.[101] There are several messages in Table 14. First there are differences between UHF and ROHF of ~200 cm^{-1} for ω_2 and ~100 cm^{-1} for ω_3 and ω_6. Second, the order of the ω_5 and ω_6 frequencies is interchanged. Third, the

Table 13 Correlated Vibrational Frequencies (cm^{-1}) and Intensities (km mol^{-1}) in Parentheses for HCN, CO_2, and C_2H_2 in a TZ2Pf Basis[a]

	HCN			CO_2			C_2H_2				
Method	$1(\sigma)$	$2(\sigma)$	$3(\pi)$	$1(\sigma_g)$	$2(\sigma_u)$	$3(\pi_g)$	$1(\sigma_g)$	$2(\sigma_g)$	$3(\sigma_u)$	$4(\pi_g)$	$5(\pi_u)$
MBPT(2)	3481	2044	726	1356	2421	659	3544	1986	3451	613	756
	(85.8)	(0.22)	(74.1)	(0)	(561.0)	(50.0)	(0)	(0)	(99.0)	(0)	(179.2)
CCSD(T)	3450	2126	723	1351	2393	663	3514	2010	3416	599	749
	(71.8)	(0.09)	(73.4)	(0)	(625.8)	(58.6)	(0)	(0)	(84.9)	(0)	(178.4)
Experimental	3440	2128	727	1354	2397	673	3497	2011	3415	624	747
	(62)	(0)	(58)	(0)	(551)	(48)	(0)	(0)	(71)	(0)	(175)

[a] Reference 99.

Table 14 Harmonic Vibrational Frequencies (Intensities) of CH_2N (DZP and TZ2P Basis)[a]

	$\omega_1(a_1)$	ω_2	ω_3	$\omega_4(b_1)$	ω_5	$\omega_6(b_2)$
UHF	3207.2 (0.6)	1606.4 (17.1)	1402.4 (0.0)	3301.0 (13.1)	1051.8 (13.6)	1012.7 (39.5)
ROHF	3235.9 (2.2)	1879.3 (1.1)	1511.7 (16.5)	3328.7 (12.6)	1067.4 (13.9)	1135.0 (33.8)
UHF-MBPT(2)	3099.9 (0.2)	2041.5 (12.0)	1430.1 (19.2)	3182.2 (8.5)	954.4 (7.5)	1153.8 (34.7)
ROHF-MBPT(2)	3100.0 (0.0)	1677.4 (3.8)	1407.5 (7.2)	3197.1 (6.8)	931.3 (6.5)	981.4 (39.4)
ROHF-MBPT(2)(TZ2P)	3079.1 (0.9)	1681.9 (5.6)	1409.6 (12.2)	3176.1 (0.7)	956.2 (9.6)	988.0 (37.3)
UHF-CCSD	3066.0 (0.5)	1693.6 (1.8)	1409.1 (8.1)	3144.8 (13.3)	952.4 (7.9)	982.8 (35.4)
ROHF-CCSD	3064.9 (0.5)	1689.3 (2.0)	1408.5 (7.8)	3143.9 (13.4)	953.1 (8.0)	979.1 (35.1)
UHF-CCSD(T)	3043.8 (0.4)	1671.1 (2.4)	1396.9 (7.6)	3121.8 (13.8)	938.3 (7.3)	963.7 (36.1)
ROHF-CCSD(T)	3041.8 (0.4)	1651.8 (3.0)	1394.2 (7.1)	3119.8 (13.8)	936.9 (7.2)	953.9 (36.1)
Experimental[b]	2820	1725	1337	3103	913	954

[a] Reference 93.
[b] Actual (nonharmonic) frequencies from reference 101.

intensity distribution between the ω_2 and ω_3 mode is vastly different. Once we have performed an MBPT(2) calculation, the UHF-MBPT(2) multiplicity is still poor ($2S + 1 = 2.203$), but ROHF-MBPT(2) does not suffer from this failing. We see drastic changes of ~400 cm^{-1} for the ω_2 mode and ~200 cm^{-1} for ω_6 between the two approaches. The usefulness of a method depends on how rapidly it converges to the full CI solution, and as we have seen, CCSD and CCSD(T) go a long way toward the full CI. From the data in Table 14, therefore, it is clear that ROHF-MBPT(2) is much closer to the CCSD and CCSD(T) results, differing by only 12–26 cm^{-1} for ω_2 and 2–27 cm^{-1} for ω_6; and intensity for ω_2 is 3.8 versus 2.0 and 3.0. Notice that the CCSD and CCSD(T) results scarcely change with the choice of reference function. The reason is that CCSD and higher CC methods benefit from the orbital property of Eq. [53], below, making the methods relatively independent of orbital choice. [This feature makes it possible to use quasi–restricted Hartree–Fock orbitals (QRHF) in CCSD calculations, when the orbitals are taken from a different system and are not at all the optimum set for the problem.] As the failing of UHF-MBPT(2) is largely due to spin contamination, we can also see this from noting that the UHF-CCSD $2S + 1 = 2.018$, which is close to a perfect doublet.

The new development of ROHF-MBPT(2) analytical Hessians offers an important tool for the theoretical description of vibrational spectra but it, too, is not a panacea. Although ROHF does not suffer from spin contamination, ROHF does tend to localize unpaired electrons in unphysical ways, which can cause it to offer a poorer reference than UHF for such problems. A case in point is the $^3\Sigma_g^-$ C_4 molecule, where UHF-MBPT(2) is superior to the ROHF-MBPT(2) description.

One final informative example is offered by the O_3 molecule. As discussed O_3 possesses resonance structures and biradical character, which usually recommends at least two reference functions in its zeroth-order description. We can expect this to be a demanding case for single reference methods,[102] although multireference methods have their own problems. These results are presented in Table 15.

The first observation is that the single determinant RHF-SCF harmonic frequencies have an average error of 19% instead of the usual ~10%. A two-reference (2R or GVB) CI would appear to offer a more correct description,[103] and, although it seems to significantly reduce the error for the symmetric stretch (ω_1) and bend (ω_2), it is still substantially in error for the asymmetric stretch (ω_3), which causes an average error of 12%. In addition, the 2R-CISD calculation gives the wrong order of the levels, having $\omega_3 > \omega_1$. The CASSCF (9 orbital, 12 electron) calculation regains the relative order while underestimating each frequency.

The usually reliable MBPT(2) method shows its customary agreement for the two symmetric stretch modes in Table 15 but badly exceeds the asymmetric stretch frequency ω_3. MBPT(4) improves on ω_3, but still overestimates its value,

Table 15 Vibrational Frequencies (cm^{-1}) of O_3 at Various Levels of Theory (DZP Basis)[a]

Method	ω_1	ω_2	ω_3
SCF	1547	859	1428
2R-CISD[b]	1234	745	1352
CASSCF[c]	1098	689	989
MBPT(2)	1167	739	2373
MBPT(4)	1123	695	1547
CCSD	1256	748	1240
CCSD + T(CCSD)	1097	685	128i (327)[d]
CCSDT-1	1076	674	680
QCISD(T)[e]	1128	697	934
CCSD(T)[f]	1129	703	976
CCSDT-2[g]	1158	712	1182
CCSDT-3[f]	1149	707	1118
CCSDT[f]	1141	705	1077
Experimental	1135	716	1089

[a] Results from reference 102 except as indicated.
[b] Reference 103.
[c] Reference 104.
[d] A nonimaginary result is obtained in a larger (5s4p2d) basis.
[e] Reference 105.
[f] Reference 106.
[g] Reference 107.

causing the wrong ordering of levels to persist. The infinite-order effects in CCSD correct the ordering and reduce the average error to be below 10%; but when estimates of triple excitations are introduced, the agreement can worsen. The noniterative triples correction CCSD + T(CCSD) even gives an imaginary frequency for ω_3 that would imply that O_3 does not have C_{2v} symmetry! Though not imaginary, the iterative CCSDT-1 method gives an unreasonably low value for ω_3. The CCSD(T) noniterative approximation to CCSDT-1 gives a much better value and the correct order, whereas the QCISD(T) approximation to CCSD(T) is slightly worse. If we add even higher order terms, which would define the iterative model, CCSDT-2, we get relatively good agreement overall, except the order of ω_3 and ω_1 is wrong. CCSDT-3 with still higher order triple contributions is good. Finally, the full CCSDT method gives excellent (too good!) agreement (< 1% error) with experimental harmonic frequencies. CCSDT is an $n^3N^5N_{it}$ procedure, so it is not yet suited to large-scale application. It is, however, the reference point for all other less expensive triple excitation approximations in CC theory, and it is clear from this example that results for difficult cases can hinge on small, usually negligible contributions. Furthermore, we expect that the DZP basis used in this study makes the CCSDT agreement with experiment partly fortuitous. Much larger basis CCSD(T) results increase the frequencies by 23, 31 and 62 cm^{-1},[108] which suggests that CCSDT in a larger basis would overshoot by a like amount.

The primary problem in O_3 seems to be that the asymmetric stretch introduces two singly excited configurations that are forbidden by symmetry from mixing into the symmetric modes.[102] This causes the multireference (nondynamic) character to be worse for asymmetric stretches. Only at very high levels of purely dynamic correlation are all these factors properly handled in O_3.

An example of the removal of the harmonic force constant approximation is a study of the quartic force field for H_2O at various CC, MBPT, and CI levels.[109,110] The energy of 18 vibrational levels are correctly described to within 18 cm^{-1}, and, with an empirical correction, to within 6 cm^{-1} at the CCSDT-1 level.[111]

PHOTOELECTRON SPECTRA

Ionization Potentials

Photoelectron spectra concern energy changes involved in the process

$$h\nu + M(Q) \rightarrow M^+(Q') + e^- + KE(e^-) \qquad [50]$$

where Q indicates the quantum state of M and Q' that for M^+, and $KE(e^-)$ is the kinetic energy of the ejected electron. For N_2 in its ground state $^1\Sigma_g^+(1\sigma_g^2 1\sigma_u^2 2\sigma_g^2 2\sigma_u^2 3\sigma_g^2 1\pi_u^4)$, Eq. [50] might correspond to removing an electron from the $1\pi_u$ orbital, the $3\sigma_g$, or any other. It usually requires X-ray energies to eject electrons from inner shell orbitals, so we usually speak of XPS or ESCA for inner shell ionization and ultraviolet photoelectron spectroscopy, UPS, using less energetic UV photons for the valence shell. The SCF independent particle model readily gives an approximate interpretation of the ionization potential for an electron via *Koopmans' theorem*.[4] This assumes that the state of the ion can be approximated by simply deleting an electron from the relevant orbital in the original SCF solution $|\text{core } 3\sigma_g 3\bar{\sigma}_g 1\pi_{u_x} 1\bar{\pi}_{u_x} 1\pi_{u_y} 1\bar{\pi}_{u_y}|$ to give, for example, either $|\text{core } 3\sigma_g 1\pi_{u_x} 1\bar{\pi}_{u_x} 1\pi_{u_y} 1\bar{\pi}_{u_y}|$ or $|\text{core } 3\sigma_g 3\bar{\sigma}_g 1\pi_{u_x} 1\bar{\pi}_{u_x} 1\pi_{u_y}|$. It is assumed that the orbitals do not change from their form in the neutral species. If we work out the energy expectation values for M and M^+ within this approximation, we find that

$$\bar{E}_M = \sum_{i=1}^{n} \epsilon_i - \sum_{i,j}^{n} \langle ij \| ij \rangle$$

$$\bar{E}_{M+} = \sum_{i=1}^{n-1} \epsilon_i - \sum_{i,j}^{n-1} \langle ij \| ij \rangle \qquad [51]$$

$$E_M - \bar{E}_{M+} = \epsilon_k = -I_p(k)$$

where ϵ_k is the orbital energy associated with orbital k in the canonical SCF approximation,

$$\mathcal{F}(1)\varphi_k(1) = \epsilon_k\varphi_k(1) \qquad [52]$$

This, in fact, gives meaning to the orbital energies of an SCF calculation and is often used as a justification for the MO (instead of valence bond) model of electronic structure.

There are two approximations in interpreting ϵ_i as the negative of an I_p: (1) the MOs for the ion are not allowed to change (i.e., there is no relaxation), and (2) there is no difference in the correlation energies of M and M^+. However, correlation will lower the energy of M relative to M^+, simply because M has one more electron to correlate with all other electrons. As a result, correlation effects will tend to increase the ionization potential. On the other hand, admitting orbital relaxation will tend to lower the energy of M^+ relative to M, diminishing the I_p. In many cases these two factors fortuitously cancel for valence electrons, with Koopmans' theorem offering a reasonably good measure of the actual I_p. However, for other cases this is untrue, and N_2 is a well-known example. From Table 16 we see that Koopmans' theorem gives the wrong order, as the lowest I_p experimentally corresponds to ionization from the $3\sigma_g$ orbital instead of the $1\pi_u$ highest occupied molecular orbital (HOMO).

For core ionization the approximate cancellation that makes Koopmans' theorem work clearly does not apply because ejecting an electron from the core causes a much greater degree of orbital relaxation error. The effect of a core electron is to decrease the effective nuclear charge (via screening) by one unit. This causes large changes in the M^+ MOs. Furthermore, correlation effects are dominated by the valence electrons. The appropriate solution for SCF treatments of core ionization requires separate SCF calculations for M and M^+, which is called ΔE_{SCF}. Such values are shown in the RHF-UHF column in Table 16. Though there is no correlation in either calculation, the core relaxation effect accounts for an enormous improvement (7.34 eV). For the valence ionizations, though, this is not as pronounced, although the results are improved over

Table 16 SCF Vertical Ionization Potentials (eV) of N_2 (5s4p1d Basis)[a,b]

Leading configuration	RHF-UHF ΔE_{SCF}	RHF-QRHF (Koopmans)	RHF-ROHF ΔE_{SCF}	Experimental
$3\sigma_g^{-1}$	15.69	17.27	15.96	15.5
$1\pi_u^{-1}$	15.34	16.78	15.42	16.8
$2\sigma_u^{-1}$	19.95	21.12	20.15	18.6
$1\sigma_g^{-1}$	419.46	426.80		409.9

[a] RHF-UHF refers to a calculation for which the ground state calculation is based on an RHF reference and the ionic state calculations on a UHF reference. RHF-QRHF indicates that the ionic calculations are based on a QRHF reference (i.e., the orbitals for the ion are the same as the neutral), and RHF-ROHF indicates that they are based on an open-shell RHF reference function.

[b] Reference 112.

Koopmans' theorem. However, the order of the ΔE_{SCF} level is still erroneous. (Much better results are offered if the core ionized state is described by a broken symmetry SCF solution that corresponds to an "atomic" 1s-type core hole, rather than ejection from the $1\sigma_g$ MO.)

To improve on both SCF approximations, correlation is essential. Such results are shown in Table 17. Note that correlation effects amount to more than 1 eV for the valence ionizations, which also corrects the order, while the effect on the core ionization is about 8 eV.

The simplest way to introduce correlation into ionization potentials is to compute $E(M)$ and $E(M^+)$ with some correlated method. (For a molecule, if the energy difference is computed at the geometry of M, we obtain vertical ionization energies; or if we allow M^+ to relax to its optimum geometry before evaluating its energy, we get adiabatic ionization energies where zero-point vibrational energy differences are ignored.) Provided the correlated method is applicable to open and closed shells, this approach has the advantage that nothing new is required to calculate ionization ionization potentials beyond that needed to evaluate energies. Because such routine, widely applicable methods are usually built on a single determinant, independent particle reference, this is usually possible for the lowest (i.e., HOMO) ionization potential of closed-shell neutral molecules, or, in fact, for any ionization from a closed-shell system where the electron is ejected from the highest orbital of a particular symmetry.

In our N_2 example, energies corresponding to ionization from the $1\pi_u$, $3\sigma_g$, or $2\sigma_u$ orbitals can readily be obtained by such an approach. The reason is that the independent particle Hartree–Fock solution for the ion, whether it is UHF or ROHF, is readily converged to such states and correlated calculations can be carried out straightforwardly. Such results for N_2 are shown in Table 17. However, it is more difficult to describe an ionized state where the electron has been ionized from an orbital of the same symmetry like the $2\sigma_g$ (or $1\sigma_g$) that is lower in energy than another, as shown in Figure 13. The reason is that it is more difficult to converge a "hole" state of the ion. Remember, Hartree–Fock methods are intended to provide the lowest possible energy for a single determinant, independent particle wavefunction. That is obtained when the SCF

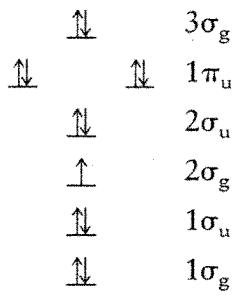

Figure 13 Orbital diagram of N_2.

Table 17 Correlated Vertical Ionization Potentials (eV) of N_2 (5s4p1d Basis)[a]

Leading configuration	RHF-UHF			RHF-QRHF			RHF-ROHF		Experimental
	CCD	CCSD	CCSDT-1	CCD	CCSD	CCSDT-1	CCSD	CCSDT-1	
$3\sigma_g^{-1}$	15.54	15.44	15.29	17.08	15.39	15.36	15.46	15.29	15.5
$1\pi_u^{-1}$	16.72	16.72	16.85	18.24	16.69	16.87	16.72	16.85	16.8
$2\sigma_u^{-1}$	18.88	18.78	18.50	20.24	18.71	18.57	18.80	18.50	18.6
$1\sigma_g^{-1}$		411.43	410.93		411.07	411.29			409.9

[a] Reference 112.

procedure interchanges orbitals $3\sigma_g$ and $2\sigma_g$, to give the $2\sigma_g^2 3\sigma_g^1$ occupancy instead, but that is just the HOMO ionized state. If this happens, we do not have an appropriate reference function to study the second ionization.

Certain algorithms can sometimes be used to force convergence to this hole state (that is how the $1\sigma_g^{-1}$ level is obtained in Tables 16 and 17), but it would be better to avoid the SCF hole state calculation altogether. In particular, it is conceptually and operationally appealing if all ionized states are described in terms of the same set of reference orbitals, namely those for the neutral, while occupying them as needed for the various possible principal ionizations. This means that we will describe the $2\sigma_g$ ionization in our example by $|\text{core}\ 2\sigma_g 2\sigma_u^2 3\sigma_g^2 1\pi_u^4|$ which we call a quasi-RHF, or QRHF wavefunction, because this is clearly not the energetically optimum determinant. This choice follows the spirit of Koopmans' theorem and does not allow the ionized state orbitals to relax.

Yet, we pointed out earlier that neglect of relaxation effects causes important errors. How do we resolve the apparent dilemma? CCSD gives us a solution. The role of $\exp(T_1)$ in CCSD and further generalizations of CCSD like CCSD(T), CCSDT-1, and CCSDT is to permit orbital rotations. That means, if we operate on a single determinant Φ_0 composed of orbitals $\varphi_1\varphi_2 \cdots \varphi_n$ we can form any other Φ_0' composed of orbitals $\varphi_1'\varphi_2' \cdots \varphi_n'$ with $\exp(T_1)\Phi_0 = \Phi_0'$. [Any Φ_0' can be obtained from Φ_0 via the action of $\exp(T_1)$, provided Φ_0' and Φ_0 are not orthogonal. This is known as the Thouless theorem.] Because the relaxed and unrelaxed orbitals are related by such an orbital rotation, we have (for CCSD),

$$\exp(T_2)\exp(T_1)\Phi_0 = \exp(T_2)\Phi_0' \qquad [53]$$

Though we never explicitly obtain Φ_0' (it could actually be constructed from the T_1 coefficients), most of the relaxation and correlation effects are introduced by solving the CCSD equations. The coupling between relaxation and correlation is incomplete until all possible excitations (i.e., those due to T_3, T_4, . . .) are also included. But CCSD is usually adequate because most correlation effects are found at just the T_2 level. This is apparent from Table 17. The difference between using the QRHF reference[112] (which is a spin eigenfunction) and the fully relaxed (but spin-contaminated) UHF reference for the ion is 0.03 to 0.07 eV for the valence levels. Even for the core, which is most sensitive to relaxation, the difference of 0.36 eV amounts to less than 0.1%!

It should be remarked that the CISD method does not share this property. The reason is that the exponential form of T_1 is critical in describing orbital rotations. Approximating $\exp(T_1)$ by $1 + T_1 = 1 + C_1$, which would be the CI form for single excitations, provides only a small part of the net effect because CI is linear and terms that are nonlinear in T_1 appear as parts of C_2, C_3, . . . , in CI approaches. Also, there is less coupling through the higher excitations because CISD, for example, would not include the T_1T_2 triple and T_2^2 quadruple excitation terms of CCSD. Similarly, no conventional finite-order perturba-

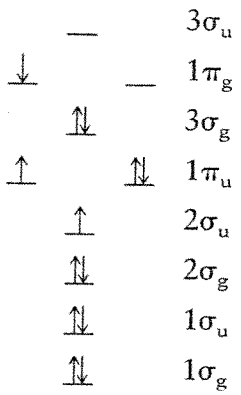

Figure 14 Example of a shake-up ionization for N_2.

tion method (even fourth-order) has a similar degree of invariance, because it is the infinite-order aspect of CC theory that is critical here. After T_2, the most important contributions come from T_3. In the N_2 example, its effect can range up to 0.5 eV. For highly accurate work, T_3 should be included and the basis should incorporate multiple polarization functions.

Before discussing even more sophisticated photoionization correlated methods, we need to mention another area in which correlation is important, namely the "shake-up" processes.[113] A shake-up ionization means that electrons are excited (or de-excited) while another is ejected, as shown in Figure 14. As the energy relative to the ground state M^+ species is changed because of excitation upon ejection of the electron, such states typically appear as satellites on the principal photoelectron peak. In a favorable case, their intensity can be comparable to that for a primary ionization. In principle, there are an infinite number of such shake-ups which correspond to each primary ionization, but only a few will be intense enough to be observable.

In the simplest unrelaxed orbital independent particle model, the energy of this particular shake-up ionization I_s (Figure 14) would be approximated by

$$I_s \approx -[\epsilon_{2\sigma_u} + \Delta E(N_2^+; \pi_u \rightarrow \pi_g)] \qquad [54]$$

where the energy required to excite an electron from the $1\pi_u$ orbital to the $1\pi_g$ orbital in the simplest model is $\Delta E = \epsilon_{1\pi_g} - \epsilon_{1\pi_u} + \langle 1\pi_g 1\pi_u \| 1\pi_g 1\pi_u \rangle$ (see later). Such a description is much less satisfactory than for principal ionizations. First, the importance of correlation is likely to be greater because there will be correlation corrections for both the excitation and the ionization process. Second, the final state for a shake-up process can involve two or more important determinants in its description. In this example, the final state corresponds to a $^2\Sigma_g$ state, but this state requires the combination of determinants that correspond to the three spatial orbitals, $1\pi_g 1\pi_u 2\sigma_u$ with $\alpha\beta\alpha$, $\beta\alpha\alpha$, $\alpha\beta\beta$, and $\beta\alpha\beta$ spins to be a proper spin eigenfunction. Furthermore, there are independent combinations that can strongly mix, causing a splitting of the shake-up state energy and making it lower than that given by the single spin combination. Hence, the single determinant description of the final state is entirely lost

as a result of final state spin symmetry considerations. The correlated wavefunction, on the other hand, can in principle introduce all such determinants, thereby permitting the proper spin-adapted combination to be constructed.

A further inadequacy of the independent particle model pertains to another kind of mixing between configurations. For example, if we ionize the $2\sigma_u$ electron and then excite a $3\sigma_g$ electron to the $3\sigma_u$ orbital, we have a second spin-adapted configuration of the same symmetry as that involving the prior $1\pi_u$-to-$1\pi_g$ excitation, which should have a comparable energy. In the absence of other restrictions, it is likely that these two configurations will strongly mix in the final state wavefunction. If so, any attempt to describe the final state as a single electron excitation is doomed to fail. Clearly, correlation is a critical component of the description of shake-up ionization processes. In the particular case discussed above, the equation-of-motion method (discussed later) gives a shake-up frequency of 30.2 eV compared to the experimental value of 30.0 eV. Obviously, we can also identify shake-ups by computing the electronic excitations for the ion using the tools for predicting electronic spectra.

The next step in the evolution of methods for photoelectron spectra is to avoid making separate calculations for the neutral species and the various possible ions. By so doing, we take advantage of certain elements of the problem that are common for each species. To do this we will use some simple operator concepts that lead us to such a set of equations.

Define R_k as an operator whose action is to create from the neutral (n electron) molecule ground state wavefunction $\Psi_0(n)$ the kth ionized state, which has $n - 1$ electrons,

$$R_k\Psi_0(n) = \Psi_0(n - 1) \qquad [55]$$

(We actually have a plane-wave continuum type orbital for the outgoing electron with energy KE that preserves the number of electrons, but we need not worry about this explicitly. This fact facilitates the commutation implicit in Eq. [59], however.) Since $\Psi_0(n)$ is a solution of the Schrödinger equation for n particles, and $\Psi_k(n - 1)$ the solution for $n - 1$ particles, we have

$$H\Psi_0 = E_0\Psi_0 \qquad [56a]$$

$$H\,R_k\Psi_0 = E_kR_k\Psi_0 \qquad [56b]$$

Multiplying Eq. [56a] by R_k, and subtracting from Eq. [56b], we then obtain

$$(H\,R_k - R_kH)\Psi_0 = I_k\Psi_0 \qquad [57]$$

where $I_k = E_k(n - 1) - E_0(n)$. In this theory, the correlated $n - 1$ electron states are described by linear combinations of single, double, etc., excitations of the $n - 1$ electron determinants starting with $\Phi_k = \mathcal{A}\,(\varphi_1(1) \cdots \varphi_{k-1}(k - 1)\ \varphi_{k+1}(k) \cdots \varphi_{n-1}(n - 1))$, made up of neutral orbitals:

$$R_k\Phi_0 = \Phi_k + \sum_{i,a} r_i^a \Phi_i^a + \sum_{\substack{i<j \\ a<b}} r_{ij}^{ab} \Phi_{ij}^{ab} + \ldots \qquad [58]$$

The objective is to determine r_i^a, r_{ij}^{ab}, etc. Now, if we choose $\Psi_0 = \exp(T)\Phi_0$, and carry out some manipulations, it may be shown that Eq. [57] can be written as

$$\bar{H}\, R_k\Phi_0 = I_k R_k \Phi_0 \qquad [59]$$

where $\bar{H} = e^{-T}\, He^T$ and $R_k\bar{H}$ turns out to vanish. Just as in ordinary CC theory, the coefficients $r_i^a, r_{ij}^{ab}, \ldots$ are determined from successive projections on single and double excitations,

$$\bar{\mathbf{H}}\mathbf{r}_k = \mathbf{r}_k I_k \qquad [60]$$

and we have for all n ionized (and shake-up) states the equation

$$\bar{\mathbf{H}}\mathbf{R} = \mathbf{R}\mathbf{I} \qquad [61]$$

where **I** is the diagonal matrix of the n ionization (and shake-up) values, and

$$\mathbf{R} = (\mathbf{r}_1, \mathbf{r}_2, \ldots, \mathbf{r}_n) \qquad [62]$$

We call this the equation-of-motion coupled cluster (EOM-CC) method.[114-116] EOM-CC results are shown in Tables 18 and 19 for CH_2PH.[117]

For principal ionization potentials, EOM-CC is equivalent to a multireference approach referred to as the Fock space multireference coupled-cluster method (FS-MRCC);[27-30] both terminologies are used. Unlike the Fock space approach, EOM-CC computational strategies also provide a way to readily obtain "shake-up" eigenvalues. Comparison of FS-MRCCSD and EOM-CCSD results with ΔE_{MBPT} and ΔE_{CC} results for CH_2PH shows excellent agreement. Results as a function of basis show improved convergence for the 5a′ level. The effect of triples as measured by the noniterative $T^*(3)$[118] is not too great.

To demonstrate results for an open-shell system, Table 20 reports results for O_2.[30] Intensities can also be obtained by considering the left eigenvector of the (non-Hermitian) operator $\bar{H}$, along with R_k, and such EOM-CC examples are shown for electronic excited states later.

Electron Affinities

Electron photodetachment experiments are not fundamentally different from photoionization; electrons are just ejected from an anion. Consequently, computing the energy for attaching an electron to a molecule $M + e^- \rightarrow M^-$

Table 18 Valence Ionization Potentials (eV) of CH_2PH Using Various Correlated Methods (DZP Basis)[a]

Orbital	MBPT(4)	CCSD	CCSDT-1	QRHF-CCSD	QRHF-CCSDT-1	EOM-CCSD	EOM-CCSD+T*(3)[b]
$1a''$	10.05	9.91	10.03	9.90	10.05	10.07	9.98
$5a'$	10.64	10.24	10.25	10.22	10.24	10.29	10.28
$4a'$				13.15	13.15	13.18	13.19
$3a'$				15.15		15.13	15.27

[a]Reference 117.
[b]Noniterative triple excitation correction. Reference 118.

Table 19 EOM-CCSD Ionization Potentials (eV) for CH_2PH as a Function of Basis Set[a]

	EOM-CCSD			
Orbital	DZ	DZP	TZP	Experimental
$1a''$	10.18	10.07	10.08	10.30
$5a'$	9.82	10.29	10.27	10.70
$4a'$	13.14	13.18	13.19	13.20
$3a'$	15.08	15.13	15.16	15.00

[a]Reference 117.

(the electron affinity, or E_A) poses many of the same methodological problems as the photoionization studies. Koopmans' theorem, ΔSCF, ΔE_{MBPT}, ΔE_{CC}, QRHF-CC or EOM-CC are all formally applicable; except that we require a description of the anion instead of the cation. There are two principal factors that make such studies more difficult:

1. An anion M^- requires a more extensive atomic basis set.
2. The extra electron in M^- introduces additional electron correlation effects.

In particular, this latter consideration makes the Koopmans estimate of E_A far worse than its estimate of a valence *I*p.

Depending on the system, the extra electron will occupy (in the independent particle description) either a partly empty valence orbital, an antibonding valence orbital, or a Rydberg orbital. In the latter two cases, a basis set chosen to describe the neutral will tend to favor M over M^-, causing E_A to be underestimated. Similarly, the additional correlation effects in M^- will tend to be underestimated at a given truncation of the FCI because higher excitation contributions will be more important. Consequently, computed E_A values are generally too small, although no rigorous bounds govern this behavior.

As an illustration consider :C=C=C=C: which is a triplet ($^3\Sigma_g^-$) with a π HOMO occupied by two electrons of parallel spin. Table 21 displays results obtained with several different levels of correlation and basis sets.[119] There are actually three different quantities that can be computed: the vertical electron detachment energy (VEDE, energy to eject electron at the geometry of the anion); the adiabatic electron affinity (AEA, when the neutral M is allowed to relax to its optimum geometry), and the vertical electron affinity (VEA, where the geometry of the neutral is assumed for the anion).

Three different experimental electron affinity values have been reported for C_4 (3.7, 3.88, and 3.79 eV). Exactly which measure of EA is being sampled is debatable, but it appears to be closest to AEA. The higher precision value of 3.88 eV would appear to offer the best comparison. Allowing for a correction of ~0.15 eV from VEDE values as obtained in the PVTZ UHF-CCSD(T) results, the larger, more diffuse basis values cluster near 3.8 eV for this quantity.

Table 20 Ionization Potentials of O_2 ($^3\Sigma_g^-$)[a]

	O_2^+			
Basis set	$^2\Pi_g$	$^4\Pi_u$	$^4\Sigma_g^-$	$^4\Sigma_u^-$
DZP	11.76	16.40	17.75	24.15
PVTZ	12.16	16.74	18.12	24.55
PVTZ++[b]	12.24	16.80	18.21	24.63
PVQZ[b]	12.34	16.90	18.31	24.71
PVQZ++[b]	12.37 (12.39)[c]	16.93 (16.76)[c]	18.34 (18.26)[c]	24.74 (24.82)[c]
Exp (vertical I_p's)[d]	12.35	16.85	18.33	24.66

[a] Reference 30.
[b] Augmented with two diffuse s and p functions.
[c] Value obtained by ΔE_{CCSD} results using UHF references for neutral and ion.
[d] Estimated vertical I_ps are extracted from adiabatic experimental values.